

Aerodynamic and dynamic loading in a blade cascade designed for flutter research

Petr Šidlof^{1*}, David Šimurda², Jan Lepicovsky², and Martin Štěpán¹

¹Technical University of Liberec, NTI FM, Studentská 2, 461 17 Liberec 1, Czech Republic

²Institute of Thermomechanics, Czech Academy of Sciences, Dolejškova 5, 182 00 Prague 8, Czech Republic

Abstract. Flow-induced vibration of turbine and compressor blades, so called blade flutter, represents a serious problem for designers and operators of large turbomachines. The research of mechanisms leading to this dangerous aeroelastic instability, which can occur especially in modern long and slender blades, is hindered by lack of experimental data. A new experimental setup for controlled flutter testing has been designed in cooperation of the Institute of Thermomechanics of the Czech Academy of Sciences and Faculty of Mechatronics of the Technical University of Liberec. The test section consists of five planar blades placed in a transonic wind tunnel, with high-frequency torsional oscillation of the middle blade driven by an electric motor. The contribution presents the results of first measurements, namely the static pressure distribution for various inlet Mach numbers, aerodynamic moments and deformation of the middle blade due to inertial loads during high-frequency oscillation.

1 Introduction

Flow-induced vibration of turbine and compressor blades, so called blade flutter, represents a serious problem for designers and operators of large turbomachines [1]. The research of mechanisms leading to this dangerous aeroelastic instability, which can occur especially in modern long and slender blades, is hindered by lack of experimental data.

Building on previous experience with the NASA Transonic Flutter Cascade [2], a new experimental setup for controlled flutter testing has been designed in cooperation of the Institute of Thermomechanics of the Czech Academy of Sciences and Faculty of Mechatronics of the Technical University of Liberec during last two years [3]. Together with numerical simulations [4], the setup will serve for investigation of the aerodynamic and structural conditions leading to this dangerous aeroelastic phenomenon. The current contribution reports on first measurements of the pressure distribution, aerodynamic moments and deformation of the middle blade due to inertial loads during high-frequency oscillation.

2 Experimental setup

2.1 Mechanical setup

The experimental setup consists of a test section, which has a width of 160 mm (along the blade span) and height 195 mm mounted in the suction-type high-speed modular wind tunnel of the Institute of Thermomechanics (see Fig. 1). The blade cascade consists of five flat blades with

rounded leading and trailing edges. The chord length of the blades is $c = 120$ mm and thickness $h = 5$ mm. The geometry of the blade cascade and location of the static pressure probes monitoring the inlet and outlet isentropic Mach number are shown in Fig. 2.



Figure 1. Test section mounted in the wind tunnel.

The incidence angles of individual blades can be varied, while the stagger angle of the entire cascade stays the same. Therefore, the torsional deformation of real blades can be readily simulated. The middle blade is driven by a high-speed electric motor and can be either fixed with a specific incidence angle, or undergo forced torsional oscillation with amplitudes 1 – 3 deg and frequencies up to 200 Hz. More details can be found in [3,4].

* Corresponding author: petr.sidlof@tul.cz

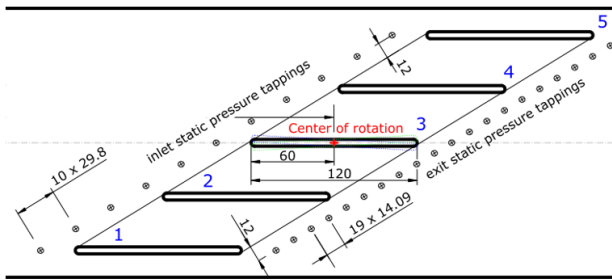


Figure 2. Geometry of the blade cascade.

2.2 Pressure, torque and motion sensors

In addition to monitoring the static pressures upstream and downstream of the blade cascade, the blades are equipped with static pressure probes, whose distribution on the blade can be seen in Fig. 3. The blade can be rotated by 180 degrees to measure the static pressure distribution both on the upper and lower surface.



Figure 3. Static pressure probes mounted in the blades.

To monitor the torque, a full strain-gauge bridge is installed on the blade drive shaft. In the case of static blades, the strain gauges measure the total aerodynamic moment. When the middle blade undergoes forced torsional oscillation, the strain gauge signal contains both the aerodynamic and inertial torque, caused by the mass (moment of inertia) of the blade.

The position and deformation of the blade during forced oscillation is measured by a laser triangulation sensor (MicroEpsilon ILD 2310-40), monitoring the vertical displacement of the leading edge in the middle of the channel.



Figure 4. Strain gauge bridges mounted on blades No. 3 and 4.

3 Results

3.1 Static pressure measurement

The results of static pressure distribution over the blade surface are reported for three different flow regimes with outlet isentropic Mach numbers ranging between $M_{2is} = 0.35 - 0.87$. In all these cases, the static incidence angle of the middle blade was $\alpha = -3^\circ$ (leading edge directed downwards). The results in Fig. 5 show a zone of low pressure on the lower surface close to the leading edge, whose value increases with the increasing flow velocity. Integration of the pressure values over the whole surface yields the total aerodynamic moment, listed in Tab. 1.

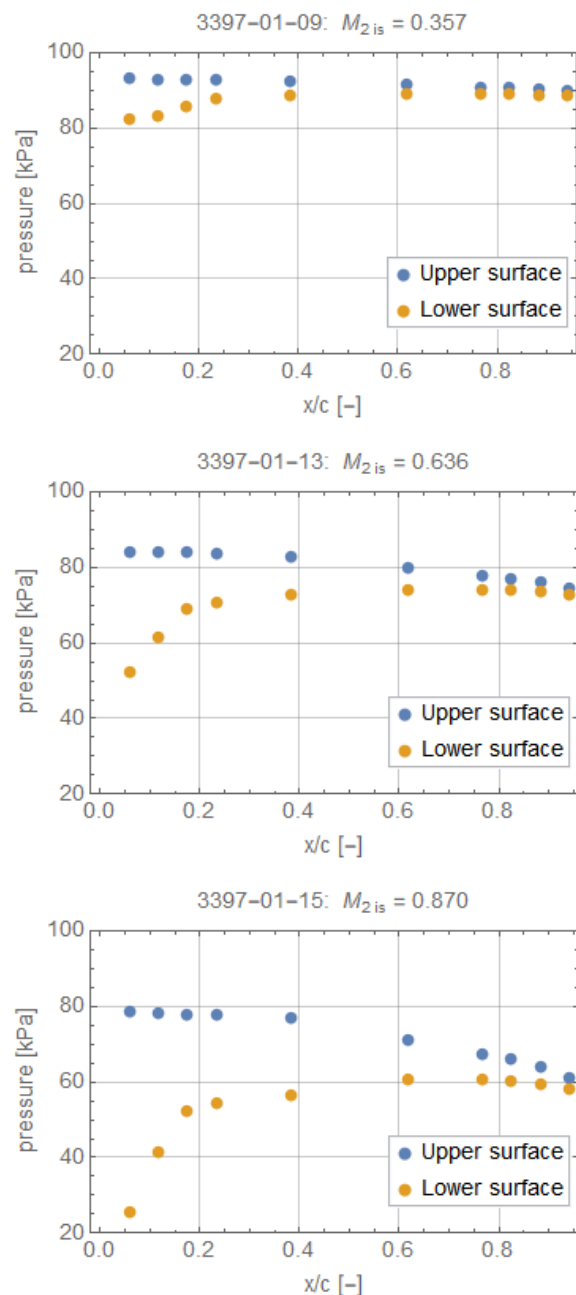


Figure 5. Distribution of the static pressure along the upper and lower surface of the middle blade for three flow regimes (values of the outlet isentropic Mach number M_{2is}).

Table 1. Aerodynamic torque on the middle blade evaluated from static pressure measurements.

ID	M1is [-]	M2is [-]	Blade static angle [deg]	Aerodynamic moment [N.m]
3997-01-09	0.3	0.357	-3	1.76
3397-01-13	0.499	0.636	-3	4.96
3397-01-15	0.596	0.870	-3	8.54

3.2 Measurement of aerodynamic torque by strain gauges

In a different set of measurements, the aerodynamic torque on the middle blade fixed with a static incidence angle $\alpha = -3^\circ$ was measured for the same three flow regimes using the full strain gauge bridge installed on the blade trunnion, as described in section 2.2. The results are summarized in Tab. 2. The data agree well both in the trend and in the order of magnitude. However, compared to the reconstructed values of aerodynamic moment in Tab. 1, the values measured by strain gauges are 30-40% lower.

Table 2. Aerodynamic torque on the middle blade measured by strain gauges for three flow regimes.

ID	M1is [-]	M2is [-]	Blade static angle [deg]	Aerodynamic moment [N.m]
3397-03	0.3	0.355	-3	1.01
3397-04	0.5	0.644	-3	3.36
3397-05	0.6	0.880	-3	5.18

3.3 Measurement of blade oscillation and inertial torque in still-air conditions

When the middle blade undergoes forced torsional oscillation, the strain gauges register not only the aerodynamic moments, but also the inertial torque. In order to assess the order of magnitude of these two components, a series of measurements was realized in still-air (zero flow velocity) conditions with a prescribed amplitude at the root of the blade $\alpha_0 = 1^\circ$ and frequency range $f = 10 - 210$ Hz. Despite the high stiffness of the structure, as the frequency increases and approaches the first natural frequency of the blade, the blade starts to twist. The waveforms and amplitudes of the leading edge deflection for increasing frequency are reported in Fig. 6.

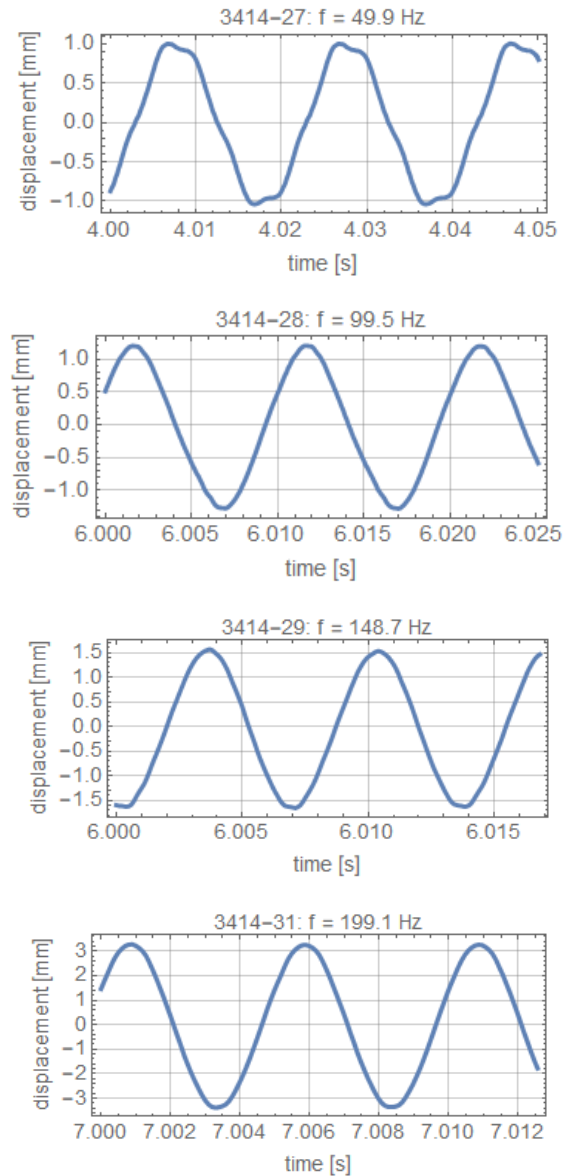
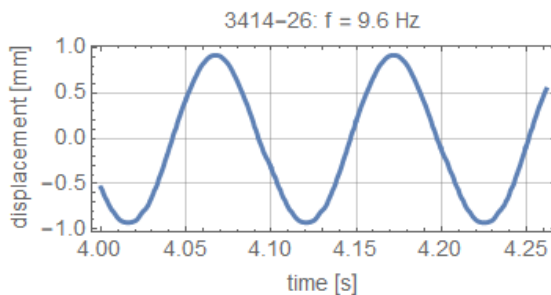


Figure 6. Deflection of the blade leading edge during oscillations in the frequency range $f = 10 - 200$ Hz.

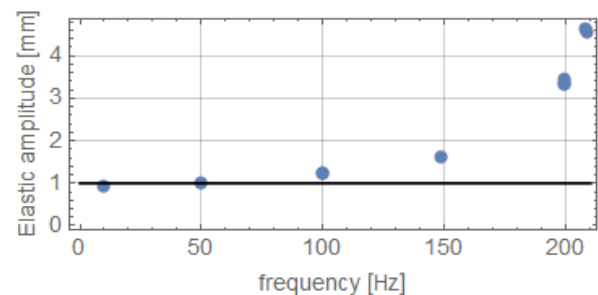


Figure 7. Amplitude of the blade oscillation measured as a function of frequency of vibration. Black line corresponds to the amplitude of a perfectly rigid blade.

For low frequency ($f = 10$ Hz), the blade oscillates as an almost perfect rigid body with an amplitude of 1 mm. At higher frequencies, however, the amplitudes sharply increase (see Fig. 7).

The signals from the strain gauge are shown in Fig. 8. For low frequencies, the torque waveform is not harmonic, which is caused mainly by the radial clearance in the driving mechanism. For higher oscillation frequencies, the inertial torque quickly increases (see also Fig. 9) and approaches the expected harmonic waveform.

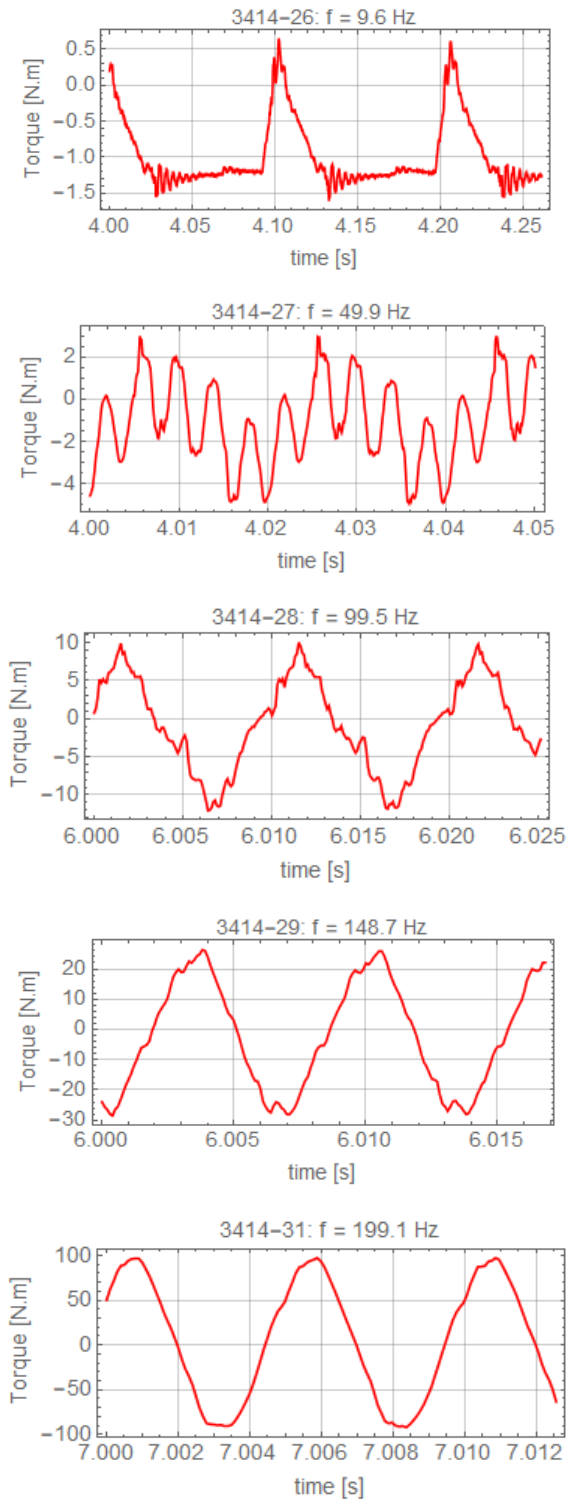


Figure 8. Torque measured by the strain gauges during oscillations in the frequency range $f = 10 - 200$ Hz in still-air conditions.

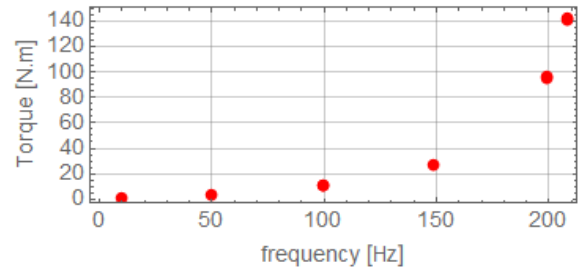


Figure 9. Amplitude of the torque as a function of frequency of vibration.

4 Discussion and conclusions

Using a new setup for blade flutter investigation, the aerodynamic moments were measured using two methods and compared to the inertial torque. In this first test, the torque measured by the strain gauges was 30–40% lower than the aerodynamic moment evaluated from static pressure measurements on the blade surface at identical flow conditions. Presumably, this was caused by inaccurate calibration of the strain gauges, and also by the fact that the number of pressure probes is limited and integration over the blade surface introduces errors.

For static incidence angles ranging between $-3^\circ \dots +3^\circ$ and outlet Mach numbers $M_{2is} = 0.3 - 0.6$, the aerodynamic moment is $1 - 6 \text{ N} \cdot \text{m}$. For lower frequencies of oscillation up to $f = 100$ Hz, this is comparable to the torque due to inertia. For higher frequencies, however, the inertial torque quickly increases and exceeds the aerodynamic moments by one or nearly two orders of magnitude. The rate of increase is higher than quadratic – this is because the frequency of the forced oscillation already approaches the lowest natural frequency of the blade. For upcoming measurements of aerodynamic moments during blade oscillation, it will be challenging to separate the inertial and aerodynamic components of the torque signal.

Acknowledgements

The research has been supported by the Czech Science Foundation, project 20-11537S “*Experimental research on flutter excitation function in turbomachinery*”.

References

1. I. McBean, K. Hourigan, M. Thompson, F. Liu, *Journal of Fluids Engineering* **127** (2005)
2. J. Lepicovsky, E.R. McFarland, V.R. Capece, T.A. Jett, R.G. Senyitko, NASA TM-211894 (2002)
3. Lepicovsky, P. Šidlof, D. Šimurda, M. Štěpán, M. Luxa, *AIP Conf. Proc.* 2323 (2021)
4. J. Fürst, M. Lasota, J. Lepicovsky, J. Musil, J. Pech, P. Šidlof, D. Šimurda, *Processes* **9**, 1974 (2021)